Nonlinear optical and optical limiting properties of graphene oxide–Fe$_3$O$_4$ hybrid material

Nonlinear optical and optical limiting properties of graphene oxide–Fe$_3$O$_4$ hybrid material

Xiao-Liang Zhang[1,2]**, Xin Zhao**[1]**, Zhi-Bo Liu**[1]**, Shuo Shi**[1]**, Wen-Yuan Zhou**[2]**, Jian-Guo Tian**[2]**, Yan-Fei Xu**[3] **and Yong-Sheng Chen**[3]

[1] The Key Laboratory of Weak Light Nonlinear Photonics, Ministry of Education,
Teda Applied Physics School, Nankai University, Tianjin 300457, People's Republic of China
[2] School of Physics, Nankai University, Tianjin 300071, People's Republic of China
[3] Key Laboratory of Functional Polymer Materials and Center for Nanoscale Science and
Technology, Institute of Polymer Chemistry, College of Chemistry, Nankai University,
Tianjin 300071, People's Republic of China

E-mail: rainingstar@nankai.edu.cn (Z-B Liu) and jjtian@nankai.edu.cn

Abstract
The nonlinear optical (NLO) and optical limiting properties of a graphene oxide hybrid material coordinated with Fe$_3$O$_4$ nanoparticles (GO–Fe$_3$O$_4$) were studied by using the Z-scan technique at 532 nm in the nanosecond and picosecond regimes. Results show that GO–Fe$_3$O$_4$ exhibits enhanced NLO and optical limiting properties in comparison with the pristine GO in the nanosecond regime. Compared with fullerene (C$_{60}$) in toluene at different concentrations, GO–Fe$_3$O$_4$ exhibits a weaker optical limiting effect than C$_{60}$ at high concentration, but shows a stronger optical limiting effect than C$_{60}$ at low concentration in the high input fluence region.

Keywords: nonlinear optics, graphene oxide, hybrid materials, Z-scan

(Some figures in this article are in colour only in the electronic version)

1. Introduction

The development of laser science and technology has motivated a lot of interest in designing optical limiters. A practical optical limiter can attenuate an optical beam strongly for high intensity or fluence, while exhibiting high transmittance for low intensity or fluence. Materials with large NLO properties can be promising candidates for optical limiting and they have attracted considerable interest in studying the NLO properties of new materials. Up to now, numerous materials, including phthalocyanines [1, 2], porphyrins [3, 4], fullerenes [5, 6], carbon nanotubes (CNTs) [7–10], inorganic nanoparticles [11, 12], graphene, and graphene oxide (GO) [13–15], have been reported to have NLO properties and optical limiting effects. Several NLO mechanisms, particularly multiphoton absorption, reverse saturable absorption (RSA),

nonlinear scattering, and nonlinear refraction have been found to dominate different kinds of NLO materials [16].

In the past few decades, great efforts have been made to promote the NLO properties by modifying the structures of the NLO materials. Recently, carbon-based hybrid materials decorated with organic dye [17–21] or semiconductor nanoparticles [22, 23] have been shown to exhibit enhanced NLO properties due to the combination of multiple NLO mechanisms and the proposed photoinduced electron or energy transfer in the hybrid materials, which provides a good approach to obtaining materials with high values for their NLO properties.

Among various graphene-base hybrid materials, GO decorated with magnetic Fe$_3$O$_4$ nanoparticles has attracted attention due to its potential application in the fabrication of functional polymer composites, sensors, waste water
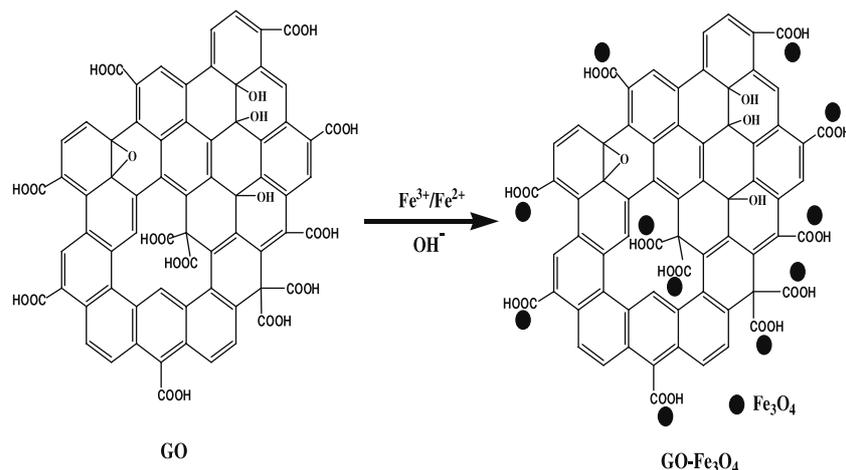
Figure 1. Scheme of the synthesis of the GO–Fe$_3$O$_4$ hybrid material.

treatment, and drug delivery [24–26]. What is more, Fe$_3$O$_4$ nanomaterials have shown strong excited state absorption and nonlinear scattering [27, 28]. Hence, it is expected that GO decorated with magnetic Fe$_3$O$_4$ nanoparticles would have high values for its NLO properties owing to a combination of nonlinear mechanisms of GO and Fe$_3$O$_4$ nanoparticles. However, there are few detailed reports on the NLO properties of this kind of hybrid material [29]. In this paper, we study the nonlinear absorption, nonlinear refraction, nonlinear scattering properties, and optical limiting effect of the GO–Fe$_3$O$_4$ hybrid material. The results show that GO–Fe$_3$O$_4$ exhibits enhanced nonlinear refraction, nonlinear scattering, and optical limiting effect compared with the pristine GO. To evaluate the NLO properties and optical limiting effect of GO–Fe$_3$O$_4$, we also compared it with the benchmark optical limiting material of fullerene C$_{60}$ in toluene.

2. Experimental section

GO was prepared from purified natural graphite according to a modified hummer method [30, 31]. The oxygen-containing groups in GO make it strongly hydrophilic and water soluble. The statistical analysis using atomic force microscopy shows that the size of GO sheets is mainly distributed between 200 and 500 nm. The synthesis of GO–Fe$_3$O$_4$ hybrid was prepared by chemical deposition of iron ions using water soluble GO as carrier, and Fe$_3$O$_4$ is bound onto the GO surface by the coordination interaction between the –COOH and Fe$_3$O$_4$ [24, 29] (as shown in figure 1). The formation of this hybrid was verified by Fourier transform infrared spectroscopy, high resolution transmission electron microscopy, and x-ray powder diffraction [29]. The size of Fe$_3$O$_4$ nanoparticles is 2–4 nm with a narrow size distribution, and some Fe$_3$O$_4$ aggregation is also observed [29].

The Z-scan experiments were conducted with a linearly polarized 5 ns and 35 ps pulsed laser at 532 nm generated from a frequency doubled *Q*-switched Nd:YAG laser (Continuum Surelite-II) and a mode-locked Nd:YAG laser (Continuum model PY61), respectively. The optical limiting experiments

were only conducted with a 5 ns pulsed laser. The pulsed laser was set at a repetition rate of 10 Hz for Z-scan and single pulse mode for optical limiting experiments. The spatial profile of the pulsed beam was of nearly Gaussian distribution after spatial filtering. The pulsed beam was split into two parts: the reflected part was used as reference, and the transmitted part was focused onto samples by using a 25 cm focal length lens. The reflected and transmitted pulses energies were measured simultaneously by using two energy detectors (PE9-SH-ROHS Ophir). In the Z-scan experiments, samples were moved along the propagation direction of the focused beam. In the optical limiting measurements, the samples were placed at the focus where the focused spot radius was about 23 μm (1/e^2); an aperture with a diameter of 8 mm was placed between the detector and the sample where all the transmitted energy could just go through it when the sample was far away from the focus. The 8 mm aperture was used to fully take advantage of negative nonlinear refraction (self-defocusing) and nonlinear scattering. All the energy through the aperture was focused into the detector by a lens. In the nonlinear scattering measurements, a small area lens was placed at an angle of 22° with respected to the Z axis to collect the scattered signals. C$_{60}$ toluene solution was employed as a reference, GO and GO–Fe$_3$O$_4$ were in water and all the samples were contained in 5 mm thick quartz cells, no nonlinear response or damage from the quartz cell was observed in our experiments.
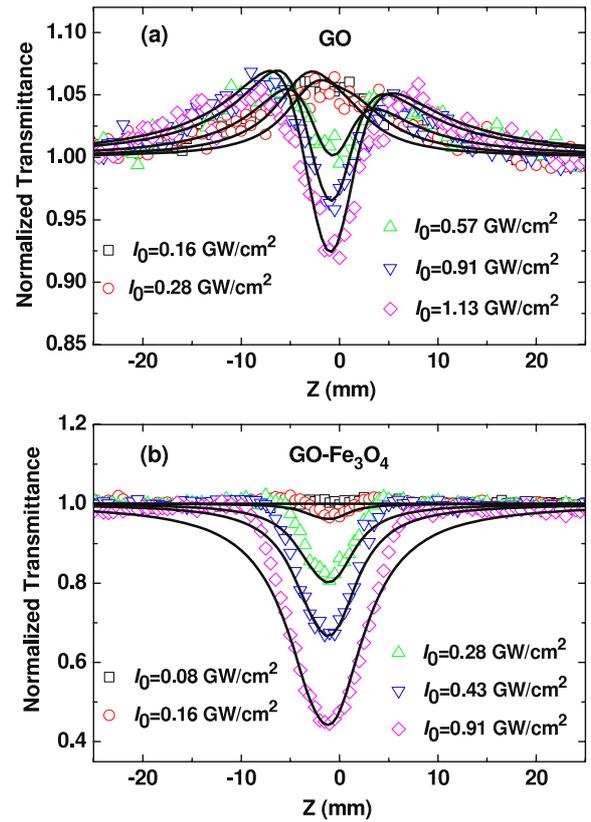
3. Results and discussion

Figure 2(a) gives the UV–visible absorption spectra of GO and GO–Fe$_3$O$_4$ in water with the same concentration of 0.033 mg ml^{-1}. GO shows a broad absorption continuously decreasing from 220 to 800 nm. Compared with GO, GO–Fe$_3$O$_4$ shows a similar broad absorption, but it exhibits weak absorption at the short wavelength region and stronger absorption at the longer wavelength region. The difference can be attributed to two factors, one is the partial removal of the epoxide and the hydroxyl groups on GO, which were deoxygenated during Fe$_3$O$_4$ nanoparticle deposition by
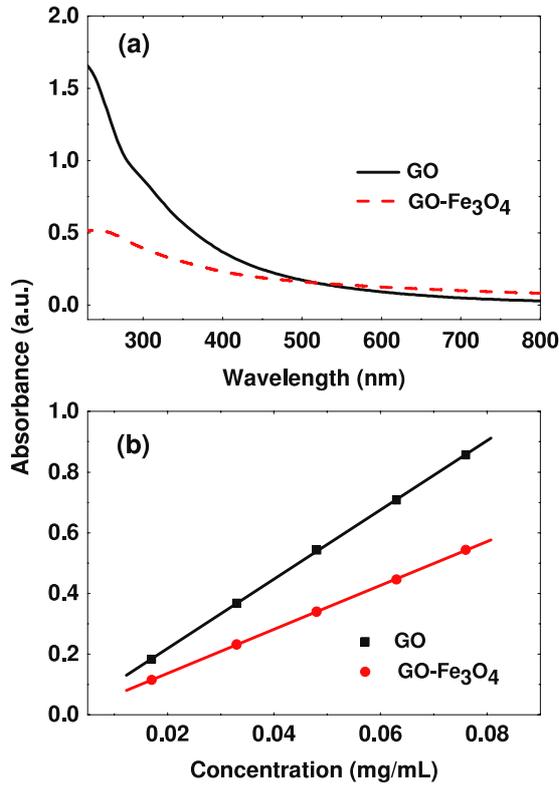
Figure 2. (a) Absorption spectra of GO and GO–Fe_3O_4 in water with the same concentration of 0.033 mg ml^{-1}. (b) The plot of absorption value at 400 nm versus concentration for GO and GO–Fe_3O_4 in water. Solid lines are linear fits.

Figure 3. Open-aperture Z-scan curves of GO (a) and GO–Fe_3O_4 (b) with the same concentration of 0.375 mg ml^{-1} at different on-axis peak intensity with nanosecond pulses. Solid lines are theoretical fits.

treating with aqueous NaOH solution [29, 32], the other is the absorption of Fe_3O_4 nanoparticles. UV–visible absorption spectra of GO and GO–Fe_3O_4 with various concentrations were also measured. To avoid the strong absorption in the UV region beyond the ability of the spectrophotometer, the concentration was controlled not to be higher than 0.08 mg ml^{-1} for the absorption spectra measurements. The absorbance values at 400 nm were plotted against concentration and are shown in figure 2(b). The observed absorption is linearly dependent on concentrations (Lambert–Beer's law) and similar results are also obtained at other wavelengths, which indicates that both GO and GO–Fe_3O_4 are dispersed homogeneously in water. Since GO–Fe_3O_4 was prepared by chemical deposition of Fe^{3+} and Fe^{2+} ions using GO as carriers and no pristine Fe_3O_4 nanoparticles were synthesized [29], Fe_3O_4 nanoparticles were not measured in our experiments.

The nonlinear optical properties of the samples were measured by the Z-scan technique [33] at 532 nm in nanosecond and picosecond regimes. Figure 3 shows the open-aperture Z-scan curves of GO, GO–Fe_3O_4 in water with the same concentration of 0.375 mg ml^{-1} at different on-axis peak intensity. As shown in figure 3, at low intensity, GO shows a symmetrical transmittance peak at the focus ($z = 0$), indicating that the saturable absorption (SA) is dominant. As intensity increases, a valley inside the peak appears at the focus and becomes deeper gradually. This implies that the RSA-like

behavior occurs similarly to the results in [13]. Unlike GO, the open-aperture Z-scan curves of GO–Fe_3O_4 exhibit only a valley at the focus, and the valley becomes increasingly deeper.

Compared with the transition from SA to RSA-like behavior of GO as input intensity increases, GO–Fe_3O_4 keeps the strong RSA-like behavior. This change can be attributed to the coordination of GO with Fe_3O_4 nanoparticles. To evaluate the NLO properties of GO and GO–Fe_3O_4 quantitatively, we fit the experimental data by solving the propagation equation of the electric field envelope E:

$$\frac{1}{r}\frac{\partial}{\partial r}\left(r\frac{\partial E}{\partial r}\right) - 2ik\frac{\partial E}{\partial z} - ik\alpha E + \frac{2k^2}{n_0}\Delta n E = 0 \quad (1)$$

$$\alpha(I) = \frac{\alpha_0}{\sqrt{1 + \frac{I}{I_S}}} + \beta_{\text{eff}} I \quad (2)$$

$$\Delta n = n_{2\text{eff}} I \quad (3)$$

where a modified nonlinear absorption coefficient $\alpha(I)$ is used to combine the SA and two-photon absorption (TPA) coefficients [34, 35], α_0 is the linear absorption coefficient, I is the laser radiation intensity, I_S is saturable intensity, n_0 is linear refraction index, $n_{2\text{eff}}$ is the effective nonlinear refraction coefficient, β_{eff} is the effective TPA coefficient and k is the wavevector. α_0 is 3.39 cm^{-1} and 3.99 cm^{-1} for GO and GO–Fe_3O_4 at 532 nm with the same concentration of
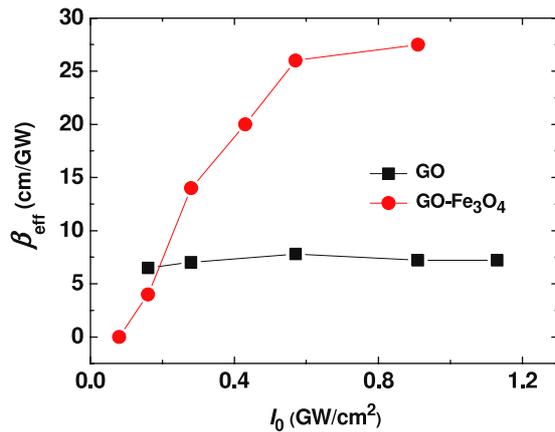
Figure 4. The values of the effective TPA coefficient β_{eff} as a function of on-axis peak intensity for GO and GO–Fe$_3$O$_4$ with the same concentration of 0.375 mg ml^{-1} in the case of nanosecond pulses.

0.375 mg ml^{-1}, respectively. For GO, $I_S = 1.2 \times 10^8$ W cm^{-2} is obtained, while I_S is near to infinity for GO–Fe$_3$O$_4$. To illustrate the difference in mechanism of NLO in GO and GO–Fe$_3$O$_4$, we give β_{eff} as a function of input intensities for the two samples, As shown in figure 4, the effective TPA coefficient β_{eff} is nearly a constant of 7 cm GW^{-1} at different input intensities for GO, indicating the dominant TPA mechanism. However, the β_{eff} increases with input intensity for GO–Fe$_3$O$_4$, which indicates that besides TPA from the GO moiety, nonlinear scattering may also play an important role, since strong nonlinear scattering signals were observed for GO–Fe$_3$O$_4$, while no nonlinear scattering signals were observed for GO during the Z-scan measurements. (GO has no nonlinear scattering, while GO–Fe$_3$O$_4$ has strong nonlinear scattering at low intensity or fluence, as shown in figure 7.)

Figure 5 shows the open-aperture and closed-aperture Z-scan results of GO and GO–Fe$_3$O$_4$ with the same intensity and concentration. For GO, the obvious peak–valley feature of the closed-aperture Z-scan curves indicates the strong negative nonlinear refraction, while the peak of the curve is seriously suppressed for GO–Fe$_3$O$_4$, suggesting that stronger nonlinear absorption/nonlinear scattering exists. By theoretical fitting, the effective TPA coefficients β_{eff} and effective nonlinear refraction coefficients n_{2eff} were obtained as 7.8 cm GW^{-1}, 9.74×10^{-14} cm^2 W^{-1} for GO and 26 cm GW^{-1}, 2.83×10^{-13} cm^2 W^{-1} for GO–Fe$_3$O$_4$, respectively. So both the effective TPA and nonlinear refraction were enhanced in GO–Fe$_3$O$_4$ compared with the pristine GO. Since the beam waist radius at focus is about 23 μm, the build-up time of the thermally induced optical nonlinearities is about 16 ns. Compared with the pulse-width of 5 ns, the thermally induced optical nonlinearities are highly transient [36]. So the observed negative nonlinear refraction should be attributed to the transient thermally induced optical nonlinearities and the intrinsic nonlinear refraction of the samples.

Three factors may contribute to the enhancement of the NLO properties of GO–Fe$_3$O$_4$. Firstly, the Fe$_3$O$_4$ nanoparticles in GO–Fe$_3$O$_4$ should have high values of their
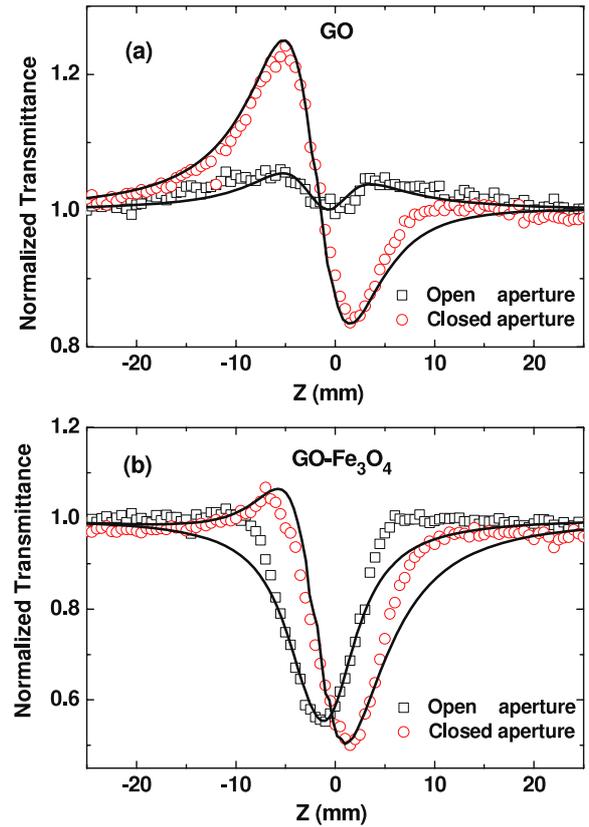
Figure 5. Open-aperture and closed-aperture Z-scan curves of GO and GO–Fe$_3$O$_4$ with the same concentration of 0.375 mg ml^{-1} at an on-axis peak intensity of 0.57 GW cm^{-2} with nanosecond pulses. Solid lines are theoretical fits.

NLO properties [27, 28]. Secondly, during the synthesis of GO–Fe$_3$O$_4$, partial reduction of GO will increase the thermal conductivity and enhance the NLO properties of GO–Fe$_3$O$_4$. In GO, epoxide and hydroxyl functional groups mostly are on the basal plane, while carboxyl groups are located at the sheet edges [37, 38]. During the synthesis of GO–Fe$_3$O$_4$, Fe$_3$O$_4$ nanoparticles mainly deposited on the edge of the GO sheet coordinated with carboxyl groups [29], while the epoxide and the hydroxyl groups on GO were partially removed by NaOH [29, 32], which increases the conjugation network of the nanostructure. The resulting integrated structure will transfer crystal lattice vibrations more rapidly, and thus the thermal conductivity of GO–Fe$_3$O$_4$ increases. This will lead to enhancement of nonlinear scattering and nonlinear refraction due to thermal effects. Thirdly, Fe$_3$O$_4$ nanoparticles deposited on GO may increase the size of the scattering center over that of the pristine GO, resulting in an enhanced nonlinear scattering.

Figure 6 gives the open-aperture Z-scan results of GO and GO–Fe$_3$O$_4$ at 532 nm with 35 ps pulse. Different from the case of a nanosecond pulse, GO–Fe$_3$O$_4$ shows weaker NLO properties than GO. Since nonlinear scattering is usually inefficient under a picosecond pulse [39], the observed weaker NLO properties of GO–Fe$_3$O$_4$ may be attributed to the nonlinear absorption mechanics (TPA and/or RSA).
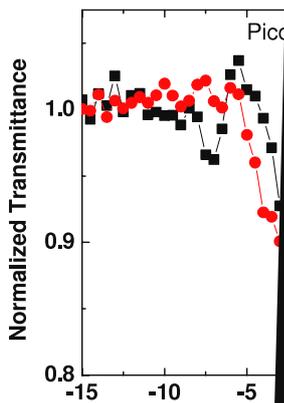
Pico

Normalized Transmittance

1.0

0.9

0.8

-15 -10 -5

Figure 6. Open-aperture Z-scan
the same concentration of 0.375

Summarizing the results
that the hybrid material GO
absorption, nonlinear refra
scattering properties, whic
limiting material under a na
has been reported to have a
is usually used as a refer
of C_{60} come from the
first singlet and t
sections than the
reported that no
play important

thresholds are 3.70 J cm^{-2}, 10.38 J cm^{-2}, and 8.58 J cm^{-2},
for GO–Fe$_3$O$_4$, GO, and C_{60}, respectively. This indicates
that GO–Fe$_3$O$_4$ shows the best optical limiting effect at low
concentration in the high input fluence region.

In our experiments, nonlinear scattering signals were also
measured for the samples. From figures 7(c) and (d), we

GO-Fe$_3$O$_4$
C_{60}
GO

10 15

t Fluence (J/c

(b)

6

5

4

T_{lin}=87%

15 20 25

ce (J/cm^2)

14
12
10
8
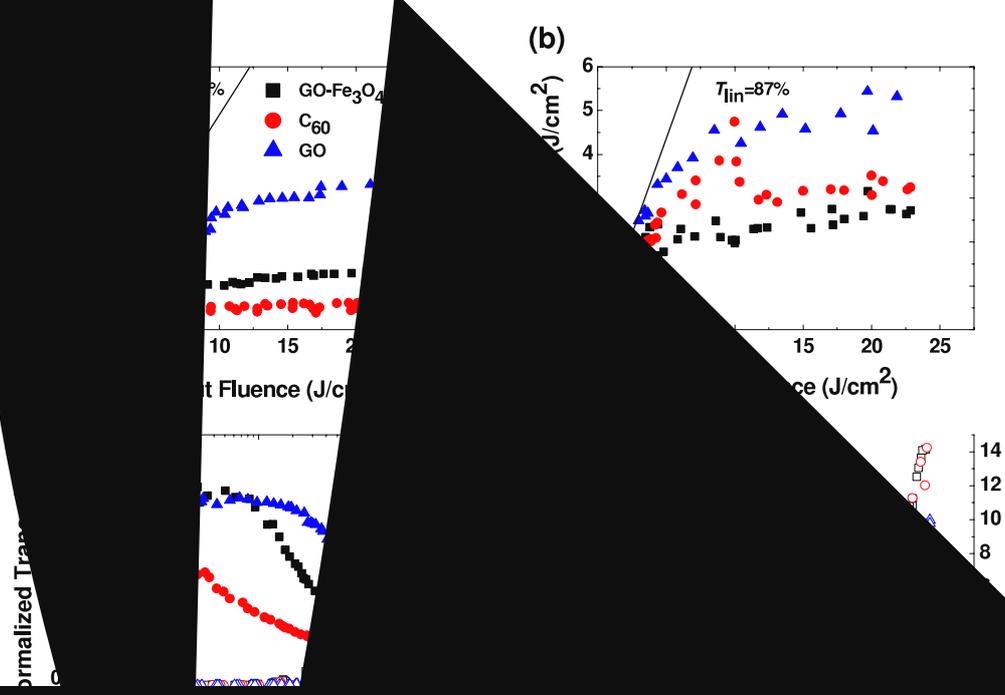
ormalized Tra

can see that the scattered intensity increase along with the decrease of normalized transmittance for the three samples at high input fluence indicate that nonlinear scattering exists and is responsible for the optical limiting at high input fluence. However, we noticed that the onset of the growth of nonlinear scattering is higher than that of the decrease of normalized transmittance, which is much more pronounced for C_{60}, indicating the existence of other nonlinear mechanisms, such as nonlinear absorption and/or nonlinear refraction. For the linear transmittance of 49% as shown in figure 7(c), we can see that GO shows the weakest scattered intensity and the weakest optical limiting effect; GO–Fe_3O_4 shows a stronger scattered intensity but weaker optical limiting effect than C_{60}. For the linear transmittance of 87% as shown in figure 7(d), C_{60} exhibits significant scattered signals and leads to the near constant output fluence for input fluence higher than $10 \, J \, cm^{-2}$, but GO–Fe_3O_4 shows a stronger scattered intensity and lower output fluence than C_{60} for input fluence higher than $2.33 \, J \, cm^{-2}$. So GO–Fe_3O_4 exhibits better optical limiting performance than C_{60} at low concentration in the high input fluence region due to the strong nonlinear scattering properties combined with negative nonlinear refraction and TPA.

A practical optical limiter requires high linear transmittance, large broadband NLO properties, and fast response time. Considering the strong scattering properties, even at low input fluence and low concentration, the strong negative nonlinear refraction, and the obvious nonlinear absorption under picosecond pulses for GO–Fe_3O_4, it is expected that the hybrid material GO–Fe_3O_4 may be a good candidate for optical limiter.

4. Conclusions

The NLO properties and optical limiting of GO and GO–Fe_3O_4 were studied. Results show that GO–Fe_3O_4 exhibits different NLO properties and enhanced optical limiting effect compared with GO. The enhanced nonlinear optical behaviors may arise from enhanced nonlinear scattering combined with TPA. GO–Fe_3O_4 exhibits larger NLO properties and stronger optical limiting effect than the benchmark optical limiting material of C_{60} at low concentration in the high input fluence region, and smaller NLO properties and weaker optical limiting effect than C_{60} at high concentration. This can be attributed to the different NLO mechanisms between GO–Fe_3O_4 and C_{60}. Since GO–Fe_3O_4 exhibits strong nonlinear optical properties and nonlinear scattering signals even at low concentration or high linear transmittance, we expect that GO–Fe_3O_4 will be an excellent candidate for broadband optical limiters.

Acknowledgments

References

[1] O'Flaherty S M, Hold S V, Cook M J, Torres T, Chen Y, Hanack M and Blau W J 2003 *Adv. Mater.* **15** 19
[2] Torre de la G, Vázquez P, Agulló-López F and Torres T 2004 *Chem. Rev.* **104** 3723
[3] Blau W J, Byrne H, Dennis W M and Kelly J M 1985 *Opt. Commun.* **56** 25
[4] Senge M O, Fazekas M, Notaras E G A, Blau W J, Zawadzka M, Locos O B and Mhuircheartaigh E M Ni 2007 *Adv. Mater.* **19** 2737
[5] Tutt L W and Kost A 1992 *Nature* **356** 225
[6] Liu C L, Zhao G Z, Gong Q H, Tang K L, Jin X L, Cui P and Li L 2000 *Opt. Commun.* **184** 309
[7] Sun X, Yu R Q, Xu G Q, Hor T S A and Ji W 1998 *Appl. Phys. Lett.* **73** 3632
[8] Vivien L, Lançon P, Riehl D, Hache F and Anglaret E 2002 *Carbon* **40** 1789
[9] Chen Y, Lin Y, Liu Y, Doyle J, He N, Zhuang X D, Bai J R and Blau W J 2007 *J. Nanosci. Nanotechnol.* **7** 1268
[10] Wang J and Blau W J 2008 *Appl. Phys.* B **91** 521
[11] Singh C P, Bindra K S, Bhalerao G M and Oak S M 2008 *Opt. Express* **16** 8440
[12] Soga D, Alves S, Campos A, Tourinho F A, Depeyrot J and Neto A M F 2007 *J. Opt. Soc. Am.* B **24** 49
[13] Liu Z B, Wang Y, Zhang X L, Xu Y F, Chen Y S and Tian J G 2009 *Appl. Phys. Lett.* **94** 021902
[14] Wang J, Hernandez Y, Lotya M, Coleman J N and Blau W J 2009 *Adv. Mater.* **21** 2430
[15] Feng M, Zhan H B and Chen Y 2010 *Appl. Phys. Lett.* **96** 033107
[16] Wang J and Blau W J 2009 *J. Opt. A: Pure Appl. Opt.* **11** 024001
[17] Xu Y F, Liu Z B, Zhang X L, Wang Y, Tian J G, Huang Y, Ma Y F, Zhang X Y and Chen Y S 2009 *Adv. Mater.* **21** 1275
[18] Liu Z B, Xu Y F, Zhang X Y, Zhang X L, Chen Y S and Tian J G 2009 *J. Phys. Chem.* B **113** 9681
[19] Zhang X L, Zhao X, Liu Z B, Liu Y S, Chen Y S and Tian J G 2009 *Opt. Express* **17** 23959
[20] Balapanuru J, Yang J X, Xiao S, Bao Q L, Jahan M, Polavarapu L, Wei J, Xu Q H and Loh K P 2010 *Angew. Chem. Int. Edn* **49** 6549
[21] Liu Z B, Tian J G, Guo Z, Ren D M, Du F, Zheng J Y and Chen Y S 2008 *Adv. Mater.* **20** 511
[22] Feng M, Sun R Q, Zhan H B and Chen Y 2010 *Nanotechnology* **21** 075601
[23] Feng M, Sun R Q, Zhan H B and Chen Y 2010 *Carbon* **48** 1177
[24] Yang X Y, Zhang X Y, Ma Y F, Huang Y, Wang Y S and Chen Y S 2009 *J. Mater. Chem.* **19** 2710
[25] Shen J F, Hu Y Z, Shi M, Li N, Ma H W and Ye M X 2010 *J. Phys. Chem.* C **114** 1498
[26] He F, Fan J T, Ma D, Zhang L M, Leung C and Chan H L 2010 *Carbon* **48** 3139
[27] Nair S S, Thomas J, Sandeep C S S, Anantharaman M R and Philip R 2008 *Appl. Phys. Lett.* **92** 171908
[28] Xing G C, Jiang J, Ying J Y and Ji W 2010 *Opt. Express* **18** 6183
[29] Zhang X Y, Yang X Y, Ma Y F, Huang Y and Chen Y S 2010 *J. Nanosci. Nanotechnol.* **10** 2984
[30] Hummers W S Jr and Offeman R E 1958 *J. Am. Chem. Soc.* **80** 1339
[31] Becerril H A, Mao J, Liu Z F, Stoltenberg R M, Bao Z N and Chen Y S 2008 *ACS Nano* **2** 463

[32] Fan X B, Peng W C, Li Y, Li X Y, Wang S L, Zhang G L and Zhang F B 2008 *Adv. Mater.* **20** 4490

[33] Sheik-Bahae M, Said A A, Wei T H, Hagan D J and Van stryland E W 1990 *IEEE J. Quantum Electron.* **26** 760

[34] Gao Y C, Zhang X R, Li Y L, Liu H F, Wang Y X, Chang Q, Jiao W Y and Song Y L 2005 *Opt. Commun.* **251** 429

[35] Gu B, Fan Y X, Wang J, Chen J, Ding J P, Wang H T and Guo B 2006 *Phys. Rev.* A **73** 065803

[36] Kovsh D I, Hagan D J and Van Stryland E W 1999 *Opt. Express* **4** 315

[37] Dikin D A, Stankovich S, Zimney E J, Piner R D, Dommett G H B, Evmenenko G, Nguyen S T and Ruoff R S 2007 *Nature* **448** 457

[38] Loh K P, Bao Q L, Ang P K and Yang J X 2010 *J. Mater. Chem.* **20** 2277

[39] Vivien L, Riehl D, Delouis J F, Delaire J A, Hache F and Anglaret E 2002 *J. Opt. Soc. Am.* B **19** 208

[40] Mishra S R, Rawat H S, Joshi M P and Mehendale S C 1994 *J. Phys. B: At. Mol. Opt. Phys.* **27** 157

[41] Justus B L, Kafafi Z H and Huston A L 1993 *Opt. Lett.* **18** 1603